AquaPack Robotics Technical Design Report

Elizabeth Gillikin*, Achyuta Kannan†, William Kelso‡, Christopher Mori‡, Bennett Petzold‡, Taylor Randall*, Donald Shrader*, Julianna White§, Robert Williamson¶

*Mechanical and Aerospace Engineering, †Computer Science
‡Electrical and Computer Engineering, § Nuclear Engineering, ¶ Biomedical Engineering

***Abstract*—AquaPack Robotics at NC State University is returning to RoboSub with SeaWolf VIII in 2024. Overall, AquaPack's goal in the 2023-2024 design cycle has been to improve and refine the reliability of the existing system. Several systems are stable, but others have required significant additional work.**

The lessons learned from the competition at TransDec in 2023 led us to another overhaul of the software system in Rust. The motivation behind this change is that this language and framework would enforce better coding practices and greater ease of use for our custom software stack. The previous Java framework proved more challenging to use than anticipated, leading to bad coding practices that saw failures at TransDec. Further systems are now fully realized such that SeaWolf VIII can attempt most of the competition course. Fully integrated manipulation systems allow for attempting torpedo and bin tasks, while the improved acoustics system allows us to attempt to surface in the octagon. Overall, this system has proven to be a stable platform suitable for continuous iteration, enabling the development of more complex systems.

Fig. 1: SeaWolf VIII

I. Competition strategy

A. General strategy: reliability and refinement

Every year, AquaPack Robotics focuses on a strategy of reliability and refinement for the current vehicle. Right now that vehicle is SeaWolf VIII. The team recognizes that a constantly changing system is unreliable, but one that never changes is subject to repeated errors. Identifying systems in acceptable condition and those needing overhaul is a must.

The 2023-2024 design cycle recognized that the electrical and mechanical systems of SeaWolf VIII were highly reliable. Continuous maintenance of these systems was prioritized over major updates. We do not imply perfect electrical or mechanical systems, but these systems have proved reliable and few difficulties arose when running SeaWolf VIII. Specific details on the current electrical and mechanical system are discussed in Sections II-B and II-A, respectively.

Software and acoustics systems demanded significant improvements. The chosen methods for software and acoustics, discussed in Sections II-D and II-G, proved challenging to develop and suffered from instabilities discovered at RoboSub 2023. For a more successful competition in 2024, these systems required refinement to the more reliable systems now deployed onto SeaWolf VIII.

B. Enter the Pacific

The competition run starts with successful navigation through the gate. Our custom-built flight controller enables six degrees of freedom locomotion, which makes navigating in a straight line through the gate and then performing a style rotation of yaw 720° achievable. Computer vision (CV) and image recognition with our front-facing camera allow us to locate and align with the gate after a random starting orientation. CV further enables us to navigate through our chosen side of the gate for additional points. This task takes the greatest priority as navigating through the gate is required to qualify.

C. Hydrothermal Vent

After successfully qualifying through gate, SeaWolf VIII interacts with the buoy. It uses its downward-facing camera to detect the Path pointing at the buoy. SeaWolf VIII aligns with the Path and navigates straight as the front-facing camera searches for the buoy. Upon detection, SeaWolf VIII circumnavigates the buoy in a direction predetermined by the software team. SeaWolf VIII has two spring-based torpedo launcher modules mounted forward-facing. SeaWolf VIII fires one torpedo at the buoy when locomotion centers it in the front-facing camera's frame. Interaction with the buoy demonstrates CV, stable locomotion, and manipulator function. All described systems are in working order, which puts the buoy as the second priority after the gate.

D. Mapping

Navigating to the torpedo task requires passive sonar. Acoustics' passive SONAR uses a Bartlett beamformer and custom register transfer language (RTL) to estimate an acoustic ping's angle of arrival (AoA). When close enough to the

target to detect, CV data takes priority for navigation and informs robot locomotion. When map detection confidence is high, SeaWolf VIII fires one of its torpedos at the general target. Due to the difficulty in navigation, reliability of operating the launchers, and accuracy of CV to align with targets, this task is of lower priority during a competition run.

E. Ocean Temperatures

The downward-facing camera on SeaWolf VIII detects the Path facing the bins. Collected images inform locomotion to center on the bin corresponding to the destination dialed. The downward-facing camera then detects the bin and drops a marker toward the open bin. This task takes priority in our strategy over torpedoes due to the reliability of our dropper system and simpler navigation that requires only the downward-facing camera.

F. Collect Samples

Once SeaWolf VIII completes all other tasks, it uses the passive sonar system to locate the octagon's pinger and the downward-facing camera to detect and align to the table in the center of the octagon. Without a grabber manipulation system, SeaWolf VIII's only task is surfacing inside to end the run.

II. Design Strategy

A. Mechanical system

The design of SeaWolf VIII, seen in Fig. 1, places an emphasis on control stability and modularity. The team built the vehicle so that fixed thrusters can achieve six degrees of freedom without relying on gimbals or hydrodynamics. The vehicle's frame construction allows for continuous mounting and modification, meeting physical needs at any time.

1) Control stability and design shape: The octagonal shape of SeaWolf VIII achieves control stability. Thrusters are farther from the center of mass, increasing their lever arm to counteract SeaWolf VIII's comparatively high mass moment of inertia. The shape, depicted in Fig. 2, has thrusters 1-4 placed in a strafe configuration. These thrusters are at 45° angles relative to the center of Sea Wolf VIII, enabling the four thrusters to all contribute to horizontal motion in any direction.

2) Modularity: A standardized hole pattern on SeaWolf VIII's frame and large bays on either side of the hull achieve modularity. The standardized hole pattern allows for easy mounting of any necessary peripheral component nearly anywhere on the robot without modification. Peripheral designs conform to the hole pattern depending on the required mounting location. The large bays on either side of the electronics hull are accessible through hinged panels, providing ample space for any new peripheral during a testing phase or final deployment. This space is also visible on either side of the central hull in Fig. 2.

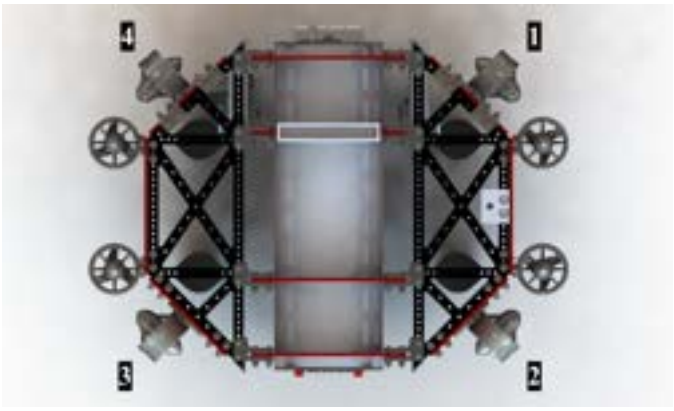

Fig. 2: Top view of SeaWolf VIII with numeric thruster labels. To either side of the central hull are empty bays for peripheral testing and mounting.

B. Electrical system

1) Main electronics board: The Main Electronics Board (MEB) is the central interface for the communications, power, and sensor systems on SeaWolf VIII via a unified I2C bus. MEB acts as the I2C controller and connects to the on-board computer. All other electrical system boards and sensors connect only to MEB as I2C followers. Thus, MEB acts as a buffer between the on-board computer and the rest of the robot. This organization enables SeaWolf VIII to effectively manage various sensors and boards situated throughout the main hull of the AUV without putting the management or computational load on the on-board computer.

2) Power System: Two 4S Lithium-polymer (LiPo) batteries power SeaWolf VIII. Each is fused at 40A, allowing a total current draw of 80A. This architecture exceeds the power demand of thrusters and the base system, ensuring power stability and room for further expansion as desired.

Safe operating conditions are paramount. SeaWolf VIII includes a load balancing circuit using ideal diode controllers to connect the two LiPo batteries in parallel safely. This load balancing circuit also provides reverse polarity protection. To further ensure safe operating conditions, the two external hulls holding the LiPo batteries each contain a standalone leak sensor module to allow early detection of any leak into the battery hulls.

After the load balancing circuit, power is provided to the system using two Solid State Relays (SSRs), System SSR and Thruster SSR. System SSR switches battery power to the entire system. When the system switches on, only MEB turns on. MEB then drives System SSR to supply power to the other systems, including the computer, electrical, acoustics, Thruster SSR, and other peripherals. Thruster SSR switches power to the thrusters. Thruster SSR is enabled only if the vehicle's computer generates a software arm signal *and* if the physical kill-switch is in the "armed" position. Importantly, the kill-switch is connected directly in series with the software arm circuitry, ensuring that electrical component failures cannot prevent the ability to kill the vehicle with the hardware switch.

Finally, various components on SeaWolf VIII require power regulation. These include the Jetson Nano, the acoustics system, and other electrical system boards. Power regulation on SeaWolf VIII uses a distributed architecture where each

board has its own regulator, allowing rapid development of boards and integration with minimal disruption to the rest of the system. The system provides a ”UBEC” (5V buck regulator) to each component that requires 5V, stepping down battery voltage. The acoustics system, USB hub, and various electrical system boards require 5V supplies. The Jetson Nano uses a more complex regulator architecture due to higher current requirements and increased sensitivity to voltage drops. First, power is regulated to 12V using a SEPIC topology regulator. This regulator can handle large voltage drops while maintaining a steady output. The 12V is regulated down to 5V using a buck topology converter. The 12V SEPIC ensures a stable power supply, given the occasional voltage drops experienced on the batteries due to thruster motion. The 5V buck is required to power the Jetson Nano directly while supplying high currents that a SEPIC could not provide.

C. Locomotion controls

Our custom control board handles vehicle locomotion. It is a custom motion controller using an Arm Cortex M4F microcontroller. It acts as a motion co-processor, allowing mission code running on the vehicle’s computer to describe motion in various high-level schemes. This co-processor design ensures the computer spends minimal processing time on motion and ensures control loop stability due to the deterministic nature of timings on the control board.

The control board uses a Quaternion-based approach similar to what can be used with a quadcopter [1]. A Quaternion-based approach allows numerically stable control of orientation in 3D space [2] without the potential for losing degrees of freedom that accompany Euler angles [3]. Added to this is a PID controller to maintain depth and tilt (pitch and roll) compensation to allow the description of motion in a partially world-relative 2D plane parallel to the surface. This approach ensures that slight pitch or roll errors do not result in unexpected motions.

This motion description also abstracts the vehicle’s nature to mission code, allowing the code to be easily used on different vehicles or in a simulator.

D. Software architecture

1) Action Tree and Technologies: The higher-level mission code that interfaces with the MEB and Control Board to execute tasks is written in Rust, using action trees. As depicted in Fig. 3, actions are defined at compile time in a tree from the starting to the ending action, with various manipulations to achieve the end state. Actions can be nested, chained, run in parallel, conditionally execute branches, and modify the execution of the action itself. Actions can perform more functions than those listed, but we primarily use those listed.

Our previous language, Java, was used in order to increase member retention due to Java’s prevalence in computer science curriculum. Java also provided more compile-time guarantees over the existing Python Robot Operating System (ROS) stack. However, the switch to Java did not increase the retention rate of software members. It also incurred a significant performance hit during competition, with increased memory leaks, startup times, and troubles interfacing with shared objects. The language change is an attempt to mitigate these issues. Our mission language needed to be agnostic of recruitment and provide more robust development and performance guarantees. Rust achieves these objectives by providing robust tooling to optimize code, a borrow checker that prevents segmentation faults during runtime, and comparable runtime speeds to C/C++. We switched our existing state machine architecture to an action tree system to more precisely craft the execution path of the mission.

The old state machine made tracing a single execution path convoluted and time-consuming. Action trees clearly define our actions and their transitions at compile time, with the ability to show various kinds of execution such as parallel, concurrent, and conditional execution. We generate tree visualizations by converting the tree structure into a Graphviz DOT file rendered as an SVG. Fig. 3 shows how this is rendered, with the ”AlwaysTrue” conditional taking the place of a conditional action that may change at runtime. These graphs are currently autogenerated with each build and published to the docs site.

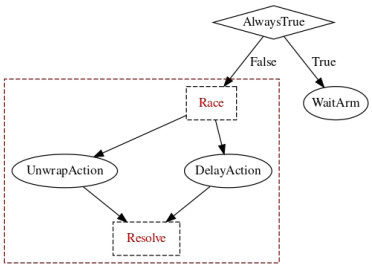

Fig. 3: Example action tree which shows a race conditional under the case of ”AlwaysTrue”.

2) Communication: A discrete communications manager handles all communication with external systems. It is allocated a static number of threads (to prevent system stalls from explosive thread growth) to send and receive messages from the control board. All serial messages generate an asynchronous task that returns true when an acknowledgment is received, allowing a wait for success. Specific messages are sent to the control board to take specific actions. The control board treats other messages as requests that return information about the robot’s current state. For example, we can command the robot to submerge to a certain depth and subsequently request its depth. This interface is abstract enough that a change to the control board would not require changes to the high-level state machine. Currently, it allows for the same communication between an actual system and simulation, with the actual system communications routed through UART and the simulation through TCP.

The system runs a GStreamer connection to share camera feeds. One pipeline offers an RTSP stream for live footage during robot testing, while another records to disk so real

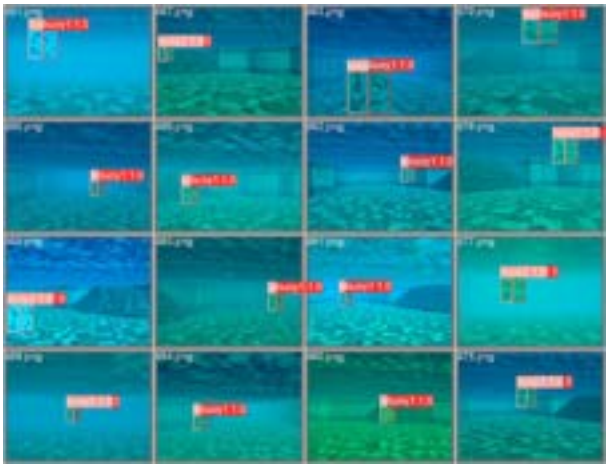

Fig. 4: Identification of Buoys in various simulated environments using ML

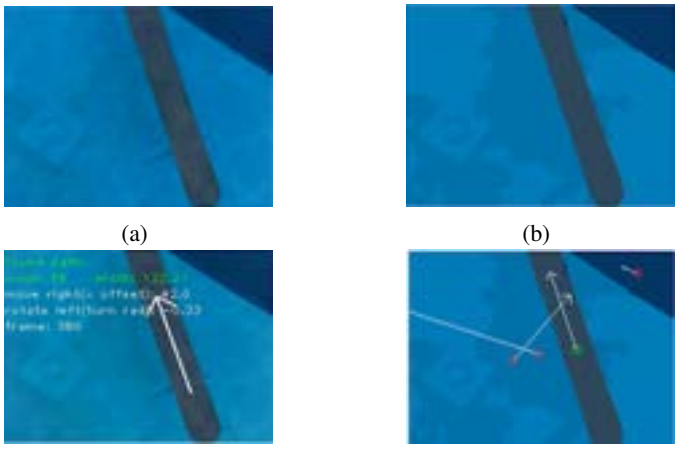

(a) (b) (c) (d)

Fig. 5: Comparison of Path-finding software in Python (a & c) and Rust (b & d)

pool images can be used for vision model testing. The vision processing code uses the last pipeline to move the robot according to the targeted game object.

3) Building, deployment, and version control: Cargo is a code management system built into Rust's build system that we use heavily. It contains code to compile and interface with Nvidia Compute Unified Device Architecture (CUDA) [4] code. Since our code is deployed onto a Nvidia Jetson Nano, we wrote scripts that cross-compile and copy the codebase onto the Jetson. Once the cross-compiled code has been deployed, the binaries run on the Jetson. Cross-compilation ensures all members can develop on their machines without worrying about deployment issues during a pool test.

All code changes are pushed to the central GitHub repository. We create branches for each new feature addition and each pool test. We have made extensive use of continuous integration to verify certain aspects of code before it is put onto the robot, such as build status and running unit tests, so that we can ensure confidence in the code we push onto the robot.

E. Computer vision

SeaWolf VIII's CV system uses classic and machine learning (ML) based approaches. Image complexity determines which approach we implement in a given mission. We implemented a classic CV approach for tasks with simple polygon shapes and a ML approach for tasks with images with complex features. Detection of the Path with classical CV is depicted in Fig. 5 with the object identified and the direction of travel shown by an arrow. Fig. 4 shows a ML identification of buoys in a simulated competition environment.

1) Classic CV: Edge and line detection is the foundational technique our classic CV uses. Edge and line detection are image processing techniques that distinguish outlines and line segments in an image. This design was referenced from software developed for RoboSub 2022, as this method worked well. We rewrote the algorithm for better integration into SeaWolf VIII's Java-based software architecture in ML-2023. Once more, we rewrote it in Rust [5] to align with our technology change. The adapted model, seen in Fig. 5, reduced images to 4 RGB colors by combining localized and global K-means to segment an image more consistently. We obtained location and directional information using Principal Component Analysis (PCA) with color and size filters to determine each color's mean and covariance.

2) ML: For images with complex features, neural networks were more suitable. They enable extracting distinct features in complex images, such as torpedo targets. We used YOLOv5 nano [6] as our model and developed a Unity [7] simulator to generate photo-realistic images of tasks to train the model, as in Fig. 4. The simulator can generate thousands of auto-labeled, synthetic images in different environments. We developed the ML model using Rust OpenCV [8] and ONNX [9] formats. We use CUDA kernels for pre and post-processing, which offloads computation from the CPU to the GPU. This offload leads to a speed-up in the overall vision pipeline since we are far from full saturation of the CUDA cores on the Jetson Nano's GPU. The CPU is thus able to process more frames per second.

F. Manipulations systems

1) Torpedo: We developed an electro-mechanical torpedo launcher system consisting of two identical launcher bodies, each housing a watertight servo motor capable of actuating a lever arm and holding a spring in compression until release. Several fused deposition modeling (FDM) printed projectiles were designed, with the chosen fusiform shape performing most favorably. Fig. 6 shows the chosen design. It is simple and it minimized the amount of electrical infrastructure needed and enabled iterative prototyping, allowing for rapid development using a FDM printer while still meeting task requirements.

2) Dropper: The dropper mechanism for SeaWolf VIII consists of three major components: a 5V electromagnet, a

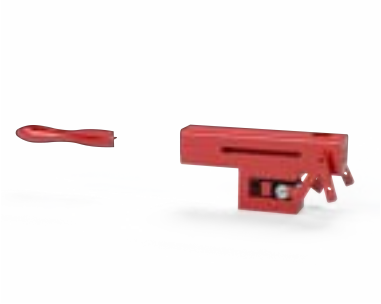

Fig. 6: SeaWolf VIII Torpedo Launcher and torpedo 3D print. Design mock-up generated in OnShape.

Fig. 7: SeaWolf VIII Dropper enclosure 3D print with the electormagnet stored internally. Design mock-up generated in OnShape.

magnetic 440C stainless steel ball, and a 3D-printed housing. The electromagnet is seated in the upper portion of the housing with a screw-on lid holding it snugly in place. The stainless steel ball, or marker, rests in the lower part of the housing. Current continuously runs through the electromagnet to create a magnetic field, which holds the marker secure in the housing. When the current stops, the marker falls straight down out of the bottom of the housing. Fig. 7 depicts one of a pair of these droppers, which are attached to the bottom of SeaWolf VIII.

G. Acoustics

Acoustic navigation via the passive SONAR system requires two central components: analog pre-processing and digital signal processing. Both components work in tandem for our acoustic system to produce reliable results for the robot to use for navigation.

1) Signal capture and pre-processing: The acoustic signal from the pingers occupies 25kHz-40kHz frequencies. This pure tone signal motivates a simple pre-processing system, which accounts for signal attenuation, white noise, and other audible frequencies. Signal capture uses a linear array of four hydrophones spaces at 2.5 cm apart. The hydrophones are phantom-powered. The system includes buffer circuitry, isolating the hydrophones from the rest of the system, and biasing circuitry, which removes the need for a negative voltage rail by using a 0dB gain op-amp circuit to change ground reference to the half supply voltage. A 10.4dB gain non-inverting op-amp circuit is used as a pre-amplifier to ensure a larger input signal capture. It is fed to four cascaded Chebyshev bandpass filters with a peak gain of 0dB or small attenuation. Without significant pass band gain in the filtering stage, the pre-amplifier becomes necessary, as small attenuation in the pass band can compromise the signal integrity of small signals captured at hydrophones. We use a digitally controlled linear amplifier, the LTC6910, for post-amplification. This stage amplifies the filtered analog waveform such that the peak-to-peak voltage occupies the entire 5V range of the analog-to-digital converters (ADC) that follow. Different amplification is necessary because path loss will change with distance by the inverse square law as we approach the pinger. The entire response of the system is depicted in Fig. II-G. The Chebyshev filter gives a steep frequency cutoff at the corner frequencies of 25 KHz and 40 KHz ensuring the only received signals are those in the band of interest that are used by RoboSub.

2) Digital signal processing: We deploy digital signal processing (DSP) on a Digilent Basys 3 FPGA develpment board. The onboard FPGA, Xilinx Artix-7, contains numerous DSP cores and several intellectual property cores that we use in development.

The base system is a Bartlett direction of arrival estimator, similar to what is described in [10]. The competition environment only has a singular signal source active at a given moment, implying that we do not need to estimate the angle of arrival for several signals in a single time window. This lends nicely to the Bartlett beamformer as it is simple to implement, but is only very successful with few signal sources [11]. The resolution of the Bartlet is also lesser than comparable direction of arrival estimators such as minimum variance distortionless response (MVDR) and multiple signal classification (MUSIC), but with only a singular source at a time, this weakness matters less, leading us to favor the Bartlett strategy which is simple to implement requiring comparably very few matrix operations.

III. Testing Strategy

A. General testing strategy

Our approach to testing our subsystems requires simulation-based and in-field testing to validate that our systems work. Simulation-based testing ensures our designs provide expected results and pinpoints flaws. In-field or pool testing validates all systems proven to operate successfully via simulation. We aimed to have at least two monthly pool tests to ensure sufficient testing of our custom control board and software architecture. Using a replica of the RoboSub course at pool tests allows the team to observe progress and re-evaluate goal timelines. See Appendix B.

B. Software and CV

Automated tests and continuous integration checks validate system functionality. Through a combination of simulation and field testing, we evaluate the performance of our software and identify areas of concern. We use simulations to train and tune our CV algorithms as described in II-E. The Unity engine [7] is

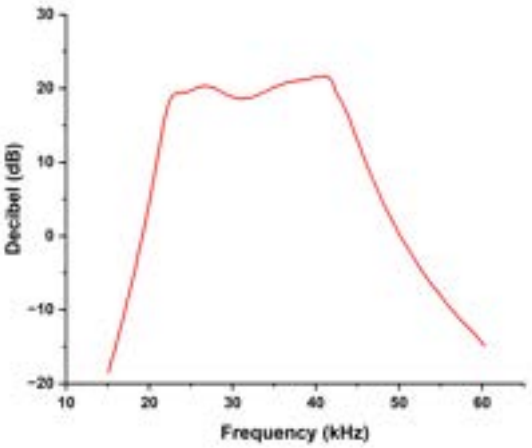

Fig. 8: Frequency Response of Analog Band Pass Filter for Passive SONAR System

our choice of simulation environment. This simulator's ability to generate thousands of photorealistic images in various environments in minutes enables a quicker turnaround for tuning our software. See Appendix B-III.

C. Manipulation

1) Torpedo: Once assembled, the torpedo system was fired repeatedly in and out of the water to ensure independent actuation of each servo and characterize projectile motion in water. This method validated the design and identified an optimal projectile shape. See Appendix B-IV.

2) Dropper: Initially, the electromagnet was installed in a 3D-printed housing and connected to a DC power supply at 5V. The electromagnet dropped the marker we placed in the housing when the manipulation system PCB applied a current to it such that it repelled the marker. This test was successful and repeatable when the dropper was out of the water. The same test with the dropper submerged in a bucket of water failed, as the marker would not deploy.

The dropper design was revised so the electromagnet would remain on and produce a magnetic field. The electromagnet stopped receiving current in this iteration, and the marker dropped. This dropper version was tested identically to the first iteration, both out of water and in the water. Both tests were successful, allowing a singular dropper to be attached to SeaWolf VIII for pool testing. Pool testing was successful, with the marker staying stable in the housing through various underwater maneuvers and deploying consistently in the pool.

D. Acoustics

All direct testing of the Acoustics system was through simulation and mathematical operation verification. Utilizing MATLAB [12], we generated sinusoidal waveforms at our sample frequency by inserting discrete additive white Gaussian noise, similar to our conditions after sampling. In code, we could directly control our time differences, giving us a benchmark for the performance of the Bartlett beamformer solution. The Bartlett beamformer proved accurate at numerous angles but would see spatial aliasing toward broadside angles.

Testing the digital backbone required simulating the Verilog code utilizing in-house-created test benches executed in the Vivado simulation environment. Testing attempted to sweep a wide range of input possibilities to give confidence that the system was robust and could withstand extremities and otherwise unpredictable randomness. Inherently, tests are limited to giving insight into how the system reacts to specific circumstances, but a large volume of testing instills the confidence in the system necessary for deployment.

IV. Acknowledgements

The AquaPack Robotics is housed within North Carolina State University's Electrical and Computer Engineering department. We would like to thank the faculty and staff who have supported and continue to support the club. Special thanks to Dr. John Muth for advising the club, as well as Casey Aquatic Center at Carmichael Gymnasium for providing us a facility for testing. Lastly, we would like to extend our gratitude to our sponsors for providing us financial support and access to their technical products for helping us design and develop the robot. Our 2023-2024 sponsors are Altium, Analog Devices Inc., BAE Systems, Caterpillar, Microsoft Corporation, NetApp, NCSU Engineer's Council, NCSU Student Government Association, NCSU Engineer Your Experience. We would also like to give a special thanks to our donors Alex Pendergast and Christopher Mori (different than the author).

References

[1] E. Fresk and G. Nikolakopoulos, "Full quaternion based attitude control for a quadrotor," 2013.

[2] B.-U. Lee, "Unit quaternion representation of rotation," Ph.D. dissertation, Stanford University, 1991.

[3] R. Pio, "Euler angle transformations," *IEEE Transactions on Automatic Control*, vol. 11, no. 4, pp. 707–715, 1966.

[4] NVIDIA, P. Vingelmann, and F. H. Fitzek, "Cuda, release: 10.2.89," 2020. [Online]. Available: https://developer.nvidia.com/cuda-toolkit

[5] N. D. Matsakis and F. S. Klock II, "The rust language," in *ACM SIGAda Ada Letters*, vol. 34, no. 3. ACM, 2014, pp. 103–104.

[6] Ultralytics, "ultralytics/yolov5: v7.0 - YOLOv5 SOTA Realtime Instance Segmentation," https://github.com/ultralytics/yolov5.com, 2022, accessed: 7th May, 2023. [Online]. Available: https://doi.org/10.5281/zenodo.7347926

[7] U. Technologies, "Unity real-time development platform: 3d, 2d, vr ar engine," accessed: 1st July, 2024. [Online]. Available: https://unity.com/

[8] Itseez, "Open source computer vision library," https://github.com/opencv/opencv, 2015.

[9] J. Bai, F. Lu, K. Zhang *et al.*, "Onnx: Open neural network exchange," https://github.com/onnx/onnx, 2019.

[10] M. Abusultan, S. Harkness, B. LaMeres, and Y. Huang, "Fpga implementation of a bartlett direction of arrival algorithm for a 5.8ghz circular antenna array," 04 2010, pp. 1 – 10.

[11] I. A. H. Adam and M. R. Islam, "Perfomance study of direction of arrival (doa) estimation algorithms for linear array antenna," in *2009 International Conference on Signal Processing Systems*, 2009, pp. 268–271.

[12] MATLAB, *version 7.10.0 (R2010a)*. Natick, Massachusetts: The MathWorks Inc., 2010.

Appendix A: Component Specifications

Component	Vendor	Model/Type	Specs	Qty.	Custom/Purchased	Cost	Year Acquired
Waterproofing							
Main Hull	OnlineMetals	8" Aluminum Tube	0.25 x 25.75 in	1	Purchased	$165.56	2022
Battery Hull	Blue Robotics	4" Watertight Enclosure	100 mm x 200 mm	2	Purchased	$638	2023
Main Hull Endcap	Mecha Inc	–	8" 6061 Aluminum	2	Purchased	$114.94	2022
Camera Enclosure	McMaster-Carr	–	–	2	Purchased & Customized	$33.2	2023
Waterproof Connector Plug	Fischer	S Series	–	22	Purchased	$750	2022
Waterproof Connector Receptacle	Fischer	DEU Series	–	22	Purchased	$750	2022
Electronic/Power System							
Load-Balancing Board (LBB): Ideal diode controllers	Digikey	LTC4359CMS8	150 µA/4V-80V	2	Purchased	$6.43	2021
Load-Balancing Board (LBB): MOSFET	Mouser Electronics	IXTN660N04T4 - I	40V/660A	2	Purchased	$32.17	2021
Main Electronics Board (MEB): Launchpad	Texas Instruments	MSP430G2553	1.8 V-3.6 V	1	Purchased		2022
LiPo Battery	Gens Ace	GEA10K4S10E5	15.2V/10000mAh/100C	2	Purchased	$154.99	2023
UBECs	SoloGood	–	5/3A Brushless Receiver Servo	3	Purchased	$12.99	2023
Manipulators							
Dropper	–	3D Printed	PETG	250g	Custom	$5.75	2023
Electromagnet	Adafruit	5V Electromagnet	5 Kg holding force	2	Purchased	$9.95	2023
Torpedo Launcher	–	3D Printed	PETG	450g	Custom	$11.50	2023
Servo Motor	Zoskay	High Torque Metal Gear Servo	25KG hold force, 6.8 V	2	Purchased	$18.36	2023
Mechanical Systems Board (MSB): Microcontroller	Texas Instruments	MSP430FR2355	16-bit/24MHz	1	Purchased	$12.99	2022
Controls							
Control Board: Microcontroller	Adafruit	ItsyBitsy	512 KB flash, 192 KB RAM32-bit Cortex M4 core	1	Purchased	$14.95	2022
Control Board: IMU	Adafruit	BNO055	9-DOF sensor, ARM Cortex-M0 based processor	8 1	Purchased	$34.95	2022
Thrusters	Blue Robotics	T200	Brushless DC motors	8	Purchased		2022
ESCs	Blue Robotics	Basic	7-26V/30A	8	Purchased	$36	2018
Acoustics							
Hydrophones	Aquarian Audio	H2C	10 Hz-100kHz Range	4	Purchased		2019
Power Distribution	–	Custom PCB Solution Rev. 2	4 Way Distribution, 1 A/Channel, 5 Vdd, 2.5 V AGND		Custom	≈$5	2022
Acoustics Front End	–	Acoustics Single Channel Rev. 1.2	500 KSps, 25kHz-40kHz BPF, 20dB-60dB passband amplification	1	Custom	≈$20	2022
Digital Signal Processing Unit	Digilent	Basys3	Xilinx Artix-7 FPGA, 90 DSP Slices, 1800 Kbits Block RAM	1	Purchased	$165	2022
Software Architecture							
Operating System	Qengineering	Ubuntu 20.04	–	–	Open-Source	$0	2022
Primary Language	Rust Foundation	Rust 1.79.0	–	–	Open-Source	$0	2022
Development Language	Python Foundation	Python 3	–	–	Open-Source	$0	2022
Serial Communication	Tokio	Tokio-serial	–	–	Open-Source	$0	2022
Automated Testing	junit-team	Junit 4.13.2	–	–	Open-Source	$0	2022
Deployment	OpenSSH	ssh	–	–	Open-Source	$0	2022
Build Tool	Rust Foundation	Cargo 0.80.0	–	–	Open-Source	$0	2022
Video Server	Gstreamer Team	Gstreamer 1.2.0	–	–	Open-Source	$0	2023
Video Processing	OpenCV	OpenCV 4.6.0	–	–	Open-Source	$0	2022
Vision							
Cameras	ArduCam	IMX219	4K 8MP	2	Purchased	$34.99	2023
OpenCV	Big Vision LLC	4.6.0	–	–	Open-Source	Open-Source	2023
YOLO	Darknet	v5	–	–	Open-Source	Open-Source	2023
Frame							
Perforated Aluminum Side 1	Custom KB Metalworks	–	8 x 10.48 x 0.250 in		Custom	Donated	2018
Perforated Aluminum Side 2	Custom KB Metalworks	–	8 x 10.48 x 0.250 in		Custom	Donated	2018
Hull Cradle	Custom KB Metalworks	–	8 x 10.48 x 0.250 in		Custom	Donated	2018
Main Hull Threaded Rod	McMaster-Carr	–	8 x 10.48 x 0.250 in		Purchased	9	2018
Interchangeable Central Platform							
Acrylic Backplane	McMaster-Carr	–	.25" Cast Acrylic	1	Purchased & Customized	$36	2023
Acrylic Truss	McMaster-Carr	–	.25" Cast Acrylic	4	Purchased & Customized	$14.40	2023
Rings	–	3D Printed	PETG	1250g	Custom	$28.74	2023

Appendix B: Test Plan and Results

I. Test Schedule

We performed seven major types of testing to debug and validate our systems. These tests included our navigation systems, manipulation systems, waterproofing measures, and full system tests. A legend of what our main protocols for simulation and testing is listed in Table I below.

TABLE I: Legend of System and Simulation Test

Test/Simulation	**Application**
Acoustics Simulation and Testing	Consists of testing how well acoustics circuits can detect and process pings in simulation and at pool tests. This helps determine if acoustics system can detect and process pings in an environment similar to the RoboSub competition.
CV Simulation	Consists of running mission and vision code through a simulated environment consisting of a pool, robot, and tasks at RoboSub. Each test consists of both running simulation and debugging. On many occasions issues found in code was debugged/improved outside of that time frame and simulated again.
Leak Tests	Consists of sealing the robot and vacuum testing its main hull and battery hulls. For each test, a pressure of -25 mm/Hg was held for a specific duration of time. Vacuum was held on the main hull for 40 minutes and each battery hull for 10 minutes. Leak tests were performed before each pool test. In the event that there appears to an issue with air leakage during a leak tests longer tests are held.
Locomotion Simulation	Consists of development and testing of simulation to validate math and orientation of custom control board. Used to identify issues with control board and correct them without in-water testing time.
Manipulation Systems Test	Consists on testing each mechanical system via its trigger to determine if system works.
Pool Tests	Consists of testing SeaWolf VIII in pool. Tests conducted at pool tests include locomotion, acoustics, CV, mission code, manipulation systems, and full system tests.
System Dry Run	Will occur before each pool test and after major changes to the electrical system have been made. Longer sessions would consist of doing checks on all of the electrical subsystems to ensure expected output was occurring. Thrusters are also run to ensure proper communication and determine if re-calibration is necessary. Typically 30 minutes each.

Table II presents the number of hours spent simulating and testing various systems and operations of SeaWolf VIII. This table includes planned hours of simulation and tests as well. Details of what each test entails is listed above in Table I.

TABLE II: Hours Spent Simulating and Testing Systems

	To-Date	**Planned**
Acoustics Simulation and Testing	20	20
CV Simulation and Testing	60	10
Leak Tests	24	3
Locomotion Simulation	50	2
Manipulation Systems Test	5.66	3
Pool Tests	68.75	21
System Dry Run	14	1.5
Total	242.41	60.5

Locomotion testing and validation was solely prioritized during the fall semester as completion of missions are not possible without proper orientation calculations and reliable communication between the control board, MEB (Main Electronics Board), and the computer. Locomotion validation was continued in the spring semester but testing of software architecture and communications was prioritized as well. Footage of props was collected for the purpose of testing simulated CV algorithms on real test cases. Summer pool tests prioritizes testing of missions and competition runs. Table III lists all completed and planned pool tests for the 2023-2024 academic year.

TABLE III: Completed and Planned Pool Test Dates

Semester	Fall	Spring	Summer
Dates	September 16th, 2023 September 30th, 2023 October 28th, 2023 November 5th, 2023	February 17th, 2024 February 24th, 2024 March 9th, 2024 March 30th, 2024 April 6th, 2024 April 13th, 2024	June 8th, 2024 June 15th, 2024 June 22th, 2024 June 29th, 2024 July 14th, 2024* July 20th, 2024* July 21th, 2024*
Hours Tested	18.25	17.5	33.75

Planned Pool Test Dates are denoted by ”*”.

II. Locomotion Testing and Validation

Proper testing of the control board is critical to mission success. However, this is a complex task requiring significant amounts of testing time during development. Due to limited in-water testing time and to ensure sufficient testing time for mission code, communications, and mechanical systems, a significant portion of control board testing occurred in simulation.

The simulator was developed using an open source 3D game engine, Godot. The selection of this tool for simulation was solely motivated by prior familiarity with this game engine. Godot includes a 3D rendering and physics engine, allowing simulator development time to focus on vehicle modeling and control board math validation.

The simulator not only models SeaWolf VIII, but simulates a control board as well. This allows testing and validation of mathematical methods in a high-level language where math libraries are already provided (by the game engine). Additionally, it allows mission code unit tests to run under simulation without access to any control board hardware or sensors.

Fig. 1: Control Board Simulator

However, a simulated control board is only capable of validating the approach to the problem, not the actual device. The largest risk with simulation testing is that the real control board's firmware has an implementation error. Even if the math is correct, it can be implemented improperly or other firmware bugs can prevent proper operation of the device. To address this, the simulator was expanded to allow use of a physical control board to control the simulated vehicle. In this operating mode, the simulator provides simulated sensor data to the control board, and receives motor speeds from the control board. Thus, the control board firmware itself can be tested and debugged under simulation.

III. ML Training and Results

Training and validation of ML algorithms is vital to their performance in detection and identification of targets. This requires an efficient and reliable environment for us to train, test, and validate our algorithms. These needs require a simulator with capabilities to support simulation of robotic systems and a powerful game engine to generate photorealistic images and environments to increase the model accuracy. As such we chose a Unity-ROS simulator as it provides sufficient support for simulating robotic systems in virtual environments and is a game engine that can produce hyper-realistic simulations.

(a) (b)

Fig. 2: Simulation of Buoys in pool environment (a) and detection of Buoys in simulated pool environment (b)

The simulation consists of images ranging from blue to blue-green for simulating various water and visibility conditions. The generation of the environment also randomizes the position and rotation of the camera and pool which challenges the algorithm to become accustomed to undesirable conditions. The training/testing/validating split of datasets used is 80-10-10.

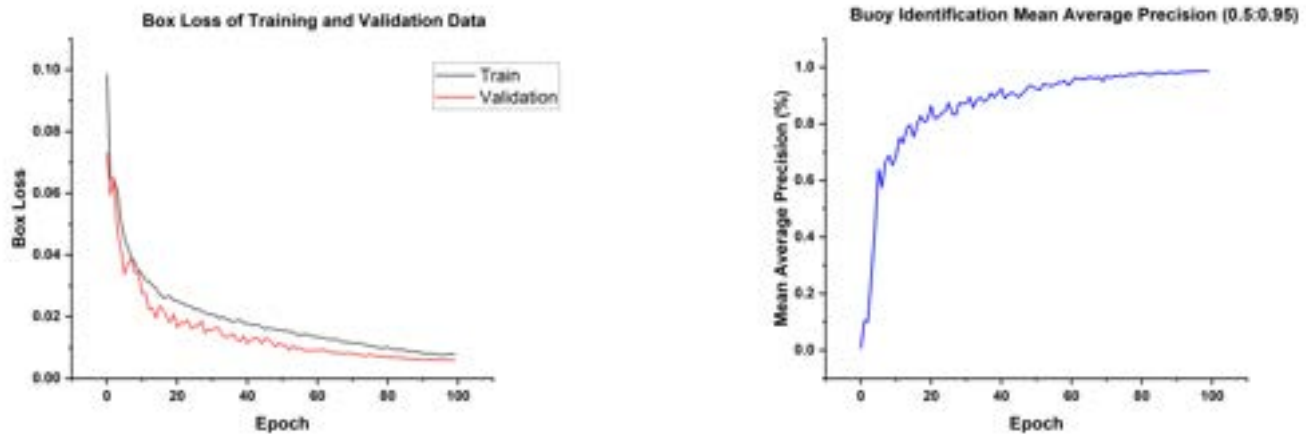

(a) (b)

Fig. 3: Box Loss of ML algorithm in training and validation data over an epoch of 100 (a) and mean average prediction of Buoys over epoch of 100 (b)

A considerable risk in developing ML models is the datasets generated oftentimes is biased to the simulated environments which results in negative performance of the algorithm in real-world conditions. The drop in performance can be associated with a simulations inability to simulate all conditions possible in the real-world which affects the neural networks ability process its input in real-world environments. To mitigate these issues, the simulator can be easily adjusted using a color slider to fit additional water conditions previously not possible. Additional assets can be added to the environment to increase variety of datasets, resulting in a more robust model. Finally, one of the best methods to mitigate a model's bias to simulated environments is incorporating real data in its training, testing, and validating datasets to improve the model's accuracy.

IV. Torpedo Projectile Test Results

Primary testing of torpedo projectile shape was through in-field testing in air and water. The test procedure included firing the assembled torpedo system and video-capture of the range of the torpedo projectile as measured by a 36 in ruler. A visual of a torpedo projectile test in water can be observed in Fig. 4.

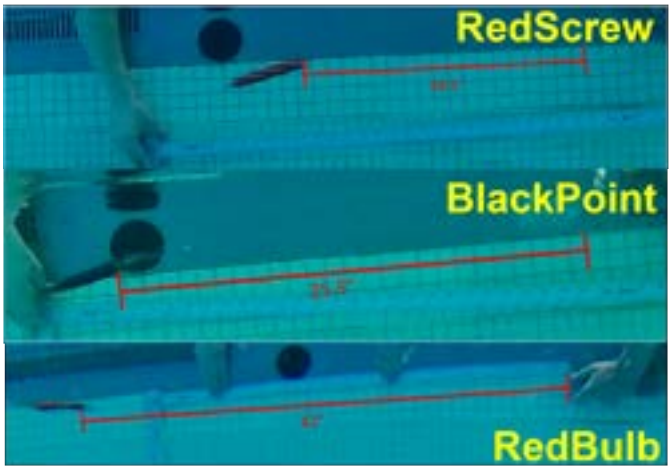

Fig. 4: Torpedo Projectile Testing

Table IV below summarizes torpedo projectile test results. Forward distance was defined as the distance the back end of the torpedo traveled away from the end of the launcher before sufficient momentum loss resulting in vertical deviation occurred. Side-to-side deviation is listed as 'minimal' if no qualitative deviation was observed.

TABLE IV: Torpedo Projectile Data

Projectile	**Avg. Forward Distance**	**Max Forward Distance**	**Side Deviation (first 30cm)**	**Side Deviation (Total)**	**Pass/Fail**
BlackPoint	23”	25.5”	Minimal	1-2”	Pass
RedScrew	17.5”	18.5”	Minimal	Minimal	Pass
RedBulb	36”	42”	Minimal	Minimal	Pass

All torpedo models met the desired minimum 12” (30cm) straight-line travel requirement with the RedBulb outperforming the other designs.